

*Engineering*

*Electrical Engineering fields*

---

Okayama University

Year 2008

---

Analysis of response mechanism of a  
proton-pumping gate FET hydrogen gas  
sensor in air

Tomiharu Yamaguchi\*      Masanori Takisawa<sup>†</sup>      Toshihiko Kiwa<sup>‡</sup>  
Hironobu Yamada\*\*      Keiji Tsukada<sup>††</sup>

\*Okayama University, [yamaguchi@sense.elec.okayama-u.ac.jp](mailto:yamaguchi@sense.elec.okayama-u.ac.jp)

<sup>†</sup>Okayama University

<sup>‡</sup>Department of Electrical and Electronic Engineering, Okayama University

\*\*Department of Electrical and Electronic Engineering, Okayama University

<sup>††</sup>Department of Electrical and Electronic Engineering, Okayama University,  
[tsukada@cc.okayama-u.ac.jp](mailto:tsukada@cc.okayama-u.ac.jp)

This paper is posted at eScholarship@OUDIR : Okayama University Digital Information  
Repository.

[http://escholarship.lib.okayama-u.ac.jp/electrical\\_engineering/119](http://escholarship.lib.okayama-u.ac.jp/electrical_engineering/119)

# Analysis of response mechanism of a proton-pumping gate FET hydrogen gas sensor in air

T. Yamaguchi, M. Takisawa, T. Kiwa, H. Yamada, K. Tsukada

*Graduate School of Natural Science and Technology, Okayama University, 3-1-1 Tsushimanaka*

*Okayama, 700-8530, JAPAN*

## **Abstract**

Two different types of hydrogen response signals (DC and AC) of a proton pumping gate FET with triple layer gate structure (Pd / proton conducting polymer / Pt) were obtained. The proton pumping gate FET showed good selectivity against other gases (CH<sub>4</sub>, C<sub>2</sub>H<sub>6</sub>, NH<sub>3</sub>, and O<sub>2</sub>). For practical use, the hydrogen response characteristics of the proton pumping gate FET were investigated in air (a gaseous mixture of oxygen and nitrogen). The proton pumping gate FET showed different hydrogen response characteristics in nitrogen as well as in air, despite the lack of oxygen interference independently. To clarify the response mechanism of the proton pumping gate FET, a hydrogen response measurement was performed, using a gas flow system and electrochemical impedance spectroscopy. Consequently, the difference in response between nitrogen and air was found to be due to the hydrogen dissociation reaction and the interference with the proton transfer caused by the adsorbed oxygen on the upper Pd gate electrode.

Keywords: Field effect transistor (FET); Hydrogen sensor; Proton pumping gate; Oxygen; Electrochemical impedance spectroscopy (EIS)

Corresponding author. Tomiharu Yamaguchi

3-1-1, Tsushima-naka, Okayama, 700-8530, JAPAN

Tel.: +81 86 251 8129; Fax: +81 86 251 8129

E-mail: yamaguchi@sense.elec.okayama-u.ac.jp

## 1. Introduction

Hydrogen energy applications have been widely studied for the generation of new energy. A hydrogen fuel cell is an environmentally-friendly and highly efficient energy source, although hydrogen gas can explode at high concentrations and cause embrittlement of storage containers. With this in mind, hydrogen gas sensors, such as those of the field effect transistor (FET) type and Schottky diode type, etc., have been reported for the detection of hydrogen leakage [1-6]. FET type hydrogen gas sensors with catalytic metal gates have sensitive and swift response properties at a low operating temperature. However, their response characteristics deteriorate at a high hydrogen concentration due to the blister formation in the palladium (Pd) used as the gate catalytic metal [7]. To solve this problem, we previously reported details of a platinum (Pt)-gate hydrogen gas sensor (Pt-FET) with stability at high hydrogen concentrations [8]. However, the gas selectivity of this FET sensor is insufficient because the gate catalytic metal of its sensor reacts to interference gases, such as methane, ethane and ammonia, meaning the gas selectivity must be improved [9, 10]. For this reason, we developed a FET type hydrogen gas sensor with a proton pumping gate (proton pumping gate FET) [11]. Because of the triple layer gate structure for the selective proton transfer, this sensor has high selectivity. In addition, the bias voltage applied between two gate electrodes can “pump” the proton to the hydrogen sensitive metal, which enables controllable sensitivity with a bias voltage. This function is useful for self-checking in multipoint or in-vehicle hydrogen sensing systems. The long-term durability of general gas sensors is one of the significant problems. These sensors detect the gas concentration using only the DC voltage signal, while this signal is affected by the output voltage drift, meaning these sensors must be periodically calibrated. In contrast, the proton pumping gate FET can distinguish the output voltage drift via the AC modulation mode, since the AC modulation signal is unaffected by the output voltage drift. However, the hydrogen sensors are generally used in air, meaning the hydrogen response characteristics in air must be investigated for practical applications. In this paper, the hydrogen response mechanism of the proton pumping gate FET in air was analyzed precisely.

## 2. Experimental

The gas sensitive layer of the proton pumping gate FET consists of an upper gate layer of Pd, a middle layer of a solid electrolyte, and a lower gate layer of Pt (Fig. 1). Nafion<sup>®</sup> was used as the solid electrolyte with proton conductivity. The base FET is an n-channel type of size 30  $\mu\text{m}$  long and 500  $\mu\text{m}$  wide. A 45 nm-thick Pt film was sputtered on the gate insulator, while 5% Nafion<sup>®</sup> solution was deposited onto the Pt gate electrode and then dried at 120°C for 10 min. A 45 nm-thick Pd film was finally sputtered on the FET gate. To analyze the response mechanism of the proton pumping gate FET, we prepared a sample with the gas sensitive layer on a glass plate. The gas sensitive layer was formed using the same procedures as those of the proton pumping gate FET, while the Nafion<sup>®</sup> layer was dried by heating at 100°C for 15 min, and the thickness of the Pd and Pt films were 30 nm and 45 nm, respectively.

The work function of the lower Pt gate electrode changes with the hydrogen adsorption on the Pt surface, which triggers the hydrogen response of the proton pumping gate FET. The work function change was measured by a voltage follower circuit (Fig. 2). This circuit supplied the proton pumping FET sensor with a constant drain current (100  $\mu\text{A}$ ) and a drain-source voltage (5 V). The lower Pt gate electrode was grounded. The work function change of the Pt gate metal was obtained as the variation in voltage between the lower gate and source of the FET. Meanwhile, DC or AC bias voltage was applied to the upper gate electrode against the lower gate. The response characteristics of the FET sensor were evaluated by the gas flow system fabricated previously [8]. The FET sensor was mounted on a ceramic substrate and the operating temperature was controlled by a heater under the flow cell. We prepared hydrogen gas at concentrations ranging from 10 ppm to 10<sup>5</sup> ppm in a nitrogen base with a one decade interval, oxygen gas at concentrations ranging from 10 ppm to 10<sup>5</sup> ppm in a nitrogen base with a two decade interval, and nitrogen gas respectively. A mixture of hydrogen and oxygen gas (oxygen gas concentration: 20%) as air was made by mixing hydrogen gas in a nitrogen base and oxygen gas. To evaluate the gas selectivity of the sensor, 0.1% and 1% concentrations of methane ( $\text{CH}_4$ ), ethane ( $\text{C}_2\text{H}_6$ ), and ammonia ( $\text{NH}_3$ ) gas in a nitrogen base were also prepared.

### 3. Results and discussion

The hydrogen response characteristics of the proton pumping gate FET were measured in a nitrogen atmosphere. When the AC rectangular bias voltage from 1 V to -1 V at 0.1 Hz was applied between the Pd and Pt gate electrodes, both DC and AC signals were obtained (Fig. 3). The DC signals ( $V_{DC1}$ ,  $V_{DC2}$ ) decreased in proportion to the logarithmic hydrogen concentration from  $10^3$  ppm to  $10^5$  ppm, as shown in Fig. 4. The hydrogen response mechanism of the conventional Pt-FET hydrogen gas sensor is based on the hydrogen dissociation reaction on the Pt electrode surface. The output voltage  $V$  of the Pt-FET sensor is expressed as the following Nernst equation [8] :

$$V = V_0 - \frac{RT}{2F} \ln P_{H_2} \quad (1)$$

where  $V_0$  is constant,  $R$  the gas constant,  $T$  the absolute temperature,  $F$  Faraday's constant, and  $P_{H_2}$  is the partial pressure of hydrogen. The DC hydrogen sensitivities of  $V_{DC1}/V_{DC2}$  (the slopes of the linear curves) were -35.8/-38.1 mV/decade at room temperature [11] and close to the theoretical value (-30 mV/decade) calculated from eq. (1). However, the sensitivities increased to -53.7/-58.7 mV/decade at 100°C and exceeded the theoretical value (-37 mV/decade) at 100°C. This result indicates that the FET proton pumping gate not only has a dissociation reaction mechanism on the lower Pt electrode but also another response mechanism, namely, the proton transfer mechanism. Protons are generated by the dissociation reaction when the hydrogen molecules adsorb on the Pd electrode. These protons diffuse into the Pd, then pass through the Nafion<sup>®</sup> layer and adsorb on the Pt gate. Consequently, the proton amount in the Nafion<sup>®</sup> layer and on the Pt electrode increases with hydrogen gas concentration. The dissociation and diffusion of protons on the Pd electrode are promoted by a rise in temperature, meaning the DC sensor sensitivities increase considerably at 100°C. In addition, the proton transfer also varies according to the AC modulation amplitude. A positive or negative electric field can promote the adsorption or desorption of the proton on the Pt electrode respectively, because the proton has a positive charge. Hence, the AC bias voltage periodically changes the

equilibrium condition of the proton adsorbed on the Pt electrode, which leads to the modulation signal. For this reason, the AC modulation signal  $V_{AC}$  of the proton pumping gate FET increases with hydrogen concentration, which triggers a greater change in  $V_{DC2}$  than  $V_{DC1}$ .

Subsequently, the hydrogen response characteristics of the proton pumping gate FET in air (an oxygen and nitrogen gas mixture) were evaluated. Figure 5 shows the DC and AC response characteristics of the proton pumping gate FET with the AC rectangular bias voltage from 1 V to -1 V at 0.1 Hz. The proton pumping gate FET was able to detect hydrogen gas at concentrations exceeding 80 ppm via the DC voltage signals. However, the decrements of the  $V_{DC1}$  and  $V_{DC2}$  were not proportional to the logarithm of hydrogen concentration. Furthermore, the AC modulation signal in air decreased at low hydrogen concentrations ranging from 8 to 800 ppm and was smaller than that in a nitrogen atmosphere. These results indicate the hydrogen gas permeation and the proton transfer of the proton pumping gate FET were affected by interference from the adsorbed oxygen on the gas sensitive layer.

We previously reported details of the oxygen interference mechanism of the Pt-FET [9]. The hydrogen response characteristic of the Pt-FET is affected by the adsorbed oxygen on the Pt electrode surface because water molecules are formed by the reaction with hydrogen and oxygen. To investigate the adsorption of interference gases on the lower Pt gate electrode, such as oxygen, methane, ethane and ammonia, the gas selectivity of the proton pumping gate FET was evaluated. The characteristics were measured in a nitrogen atmosphere. The proton pumping gate FET did not react to oxygen gas. Additionally, the proton pumping gate FET scarcely reacted to various interference gases, such as methane, ethane, and ammonia (Table 1). Although the response of the proton pumping gate FET to these gases increased with temperature, the voltage change was negligible compared to the hydrogen sensitivity (about -50 mV/decade at 100°C). These results indicate that interference gases cannot adsorb on the Pt gate layer of the proton pumping gate FET. The gas selectivity of the proton pumping gate FET is related to the gas permeation blocking. The upper Pd gate layer of the proton pumping gate FET prevents the permeation of interference gases by gas adsorption. In the case of the oxygen gas

adsorption, although oxygen molecules dissociate on the Pd layer and are negatively charged by the ionization, the permeation of these gases and ions to the lower electrode can be blocked because of the cation permeable Nafion<sup>®</sup>. However, the interference gases will partially pass through the Pd gate and reach the Nafion<sup>®</sup> layer. Thus, ammonia gas can dissolve in water contained in the Nafion<sup>®</sup> and become ammonium ions, which may result in the modest ammonia response at 100°C.

Based on the results of the hydrogen response characteristics in air and the gas sensitivity, the following was assumed regarding the response mechanism of the proton pumping gate FET in air. Oxygen gas molecules do not dissociate on the lower Pt electrode, but on the upper Pd electrode. Adsorbed hydrogen atoms react with oxygen on the Pd electrode and water molecules are formed. These water molecules desorb from its electrode or are supplied in the Nafion<sup>®</sup> layer, which prevents the adsorption of the proton on the Pt electrode. The DC response in air therefore decreases at low hydrogen concentrations. In addition, the AC signal amplitude in air also decreases compared to that in a nitrogen atmosphere because the water formation reaction reduces the protons transferred to the Nafion<sup>®</sup> layer. Meanwhile, the water molecules supplied in the Nafion<sup>®</sup> bulk increase the proton mobility in the same, which promotes proton transfer to the Pd gate at the negative bias voltage and the water formation on its gate. As a result, the intrinsic proton in the Nafion<sup>®</sup> and on the Pt gate decreases with increasing hydrogen concentration, which triggers the AC signal change in air. However, the FET proton pumping gate may still have a further response mechanism in air, meaning more research must be done to clarify this mechanism.

To analyze the response mechanism in more detail, the impedance characteristics of the proton pumping gate structure were evaluated by the electrochemical impedance spectroscopy. The glass sample with the gas sensitive layer was placed in the flow cell and the electrodes of the sample were connected to the potentiostat (Iviumstat, Ivium Technologies). The amplitude of the applied voltage was 1 V and the frequency was changed from 1 Hz to 1 MHz. As shown in Fig. 6, the Nyquist plots of the impedance described two semicircles and radii of the

semicircles changed with hydrogen concentration. These results indicate the bulk and interface impedances contribute to the AC hydrogen response of the proton pumping gate FET. The conductivity of the proton conducting polymer depends on the proton amount and the water molecules contained in its polymer, meaning the conductivity of its polymer increases with the proton transfer. Furthermore, the measured impedance data was fitted into the equivalent circuit. The figure inserted in Fig. 6 shows the general equivalent circuit of a metal/solid electrolyte/metal sandwich structure.  $R_1$  and  $C_1$  represent the bulk resistance and capacitance of the proton conducting polymer, while  $R_2$  and  $C_2$  are the interface resistance and capacitance between the electrode and the proton conducting polymer. All the parameters in the equivalent circuit were used for the simulation. The capacitance is not often ideal due to the electrode roughness and varying coating thickness, etc. Thus, the constant phase element (CPE) was placed instead of the capacitance. The CPE impedance is expressed as follows:

$$Z = \frac{1}{T(j\omega)^n} \quad (2)$$

where  $j$  is the imaginary unit,  $T$  and  $n$  constant, and  $\omega$  the frequency of the applied voltage. When  $n=1$ , the CPE behaves as an ideal capacitance element. The measured data correlated well to the equivalent circuit with the CPE elements. However,  $n$  was equal to about 0.8 and the bulk capacitance was smaller by only one order of magnitude of the interface capacitance, which may be due to partial contacts formed between the electrodes or the roughness of electrode surfaces. Figures 7 and 8 show the hydrogen concentration dependence of the resistance calculated from the fitting. Here,  $R$  is the bulk or interface resistance and  $R_0$  is the initial resistance value with only a nitrogen gas flow. In a nitrogen atmosphere, both the interface and bulk resistances decreased with increasing hydrogen concentration, which indicates hydrogen dissociation on the electrodes and the proton amount increased by proton transfer. This result corresponds to the response characteristics of the proton pumping gate FET. However, the resistance changes in air, and the interface resistance in particular remained almost unchanged at a low hydrogen concentration, meaning obvious interference with the proton transfer by the



water formation reaction. In addition, the bulk resistance decreased sharply in high hydrogen concentrations. This suggests that the dissolution of water molecules increases proton mobility in the Nafion<sup>®</sup> bulk and several protons were transferred to it, which triggers the DC and AC hydrogen response of the FET proton pumping gate in air. Based on these results, the oxygen interference with the hydrogen response in air was clarified.

#### **4. Conclusion**

The response characteristics of the proton pumping gate FET were investigated in detail. The proton pumping gate FET was able to detect hydrogen gas ranging from 80 to 8000 ppm in air via the DC signals. This indicates this sensor is sufficiently sensitive to detect hydrogen leakage in air. In addition, the AC signal of this sensor changed in low hydrogen concentrations, which enables self-checking of the output voltage drift for practical applications such as multipoint or in-vehicle hydrogen sensing systems. However, this response characteristic differed from that in a nitrogen atmosphere, because the hydrogen dissociation reaction and proton transfer were interfered with by the adsorbed oxygen on the upper Pd gate electrode. Based on the gas selectivity and the impedance measurement, the oxygen interference with the hydrogen response in air was clarified.

## References

- [1] I. Eisele, T. Doll, M. Burgmair, Low power detection with FET sensors, *Sens. Actuators B: Chem.* 78, (2001) 19-25.
- [2] M. Burgmair, H.-P. Frerichs, M. Zimmer, M. Lemann, I. Eisele, Field effect transducers for work function gas measurements: device improvements and comparison of performance, *Sens. Actuators B: Chem.* 95, (2003) 183-188.
- [3] K. Scarnagl, A. Karthigeyan, M. Burgmair, M. Zimmer, T. Doll, I. Eisele, Low temperature hydrogen detection at high concentrations: comparison of platinum and iridium, *Sens. Actuators B: Chem.* 80 (2001) 163-168.
- [4] C. K. Kim, J. H. Lee, Y. H. Lee, N. I. Cho, D. J. Kim, A study on a platinum-silicon carbide Schottky diode as a hydrogen gas sensor, *Sens. Actuators B: Chem.* 66, (2000) 116-118.
- [5] F. Raissi, R. Farivar, Room-temperature hydrogen gas sensor, *Appl. Phys. Lett.* 87, (2005) 164101.
- [6] C.-C. Cheng, Y.-Y. Tsai, K.-W. Lin, H.-I. Chen, W.-H. Hsu, C.-W. Hong, W.-C. Liu, Characteristics of a Pd-oxide-In<sub>0.49</sub>Ga<sub>0.51</sub>P high electron mobility transistor (HEMT)-based hydrogen sensor, *Sens. Actuators B: Chem.* 113, (2006) 29-35
- [7] K. Tsukada, T. Kiwa, T. Yamaguchi, K. Yokosawa, Hydrogen reaction of characteristics of FET sensors with catalytic metal gate in high hydrogen concentration, *Proc. of the 11th international meeting on chemical sensors (2006)*
- [8] K. Tsukada, T. Kiwa, T. Yamaguchi, S. Migitaka, Y. Goto, K. Yokosawa, A study of fast response characteristics for hydrogen sensing with platinum FET sensor, *Sens. Actuators B: Chem.* 114, (2006) 158-163.
- [9] T. Yamaguchi, T. Kiwa, K. Tsukada, K. Yokosawa, Oxygen interference mechanism of platinum-FET hydrogen gas sensor, *Sens. Actuators A: Phys.* 136, (2007) 244-248
- [10] T. Kiwa, T. Yamaguchi, S. Nakada, K. Yokosawa, K. Tsukada, Humidity effect on the properties of FET-type hydrogen sensors, *Proc. of the 11th international meeting on chemical sensors (2006)*

[11] K. Tsukada, T. Yamaguchi, T. Kiwa, A proton pumping gate field effect transistor for a hydrogen gas sensor, IEEE Sensors Journal 7, (2007) 1268-1269.

## **Biography**

Tomiharu Yamaguchi was born in Hyogo, Japan in 1982. He received the B.S. and M.S. degrees from Okayama University in 2005 and 2006, respectively. He is now a PhD student at Okayama University. His subject includes micro gas sensor.

Masanori Takisawa was born in Okayama, Japan in 1984. He received the B.S. degree from Okayama University in 2007. He is now a PhD student at Okayama University. His subject includes micro gas sensor.

Toshihiko Kiwa was born in Nara, Japan in 1976. He received Dr. Eng. Degree from Osaka University in 2003. After that he worked for one year as a JSPS fellow at the Research Center for Superconductor Photonics, Osaka University, where he was involved in the development of terahertz and superconductor devices. Currently, he is a Senior Assistant Professor of Department of Electrical and Electronic Engineering, Okayama University. His research interests include chemical sensors, magnetometric sensors, and terahertz devices.

Hironobu Yamada was born in Miyagi, Japan in 1977. He received Dr. Eng. Degree from Yamagata University in 2005. After that he worked for one year as a post doctoral fellow at the Institute for Materials Research, Tohoku University. Currently, he is an Assistant Professor of Department of Electrical and Electronic Engineering, Okayama University. His research interests include measurement systems engineering.

Keiji Tsukada was born in Kumamoto, Japan in 1954. He received Dr. Eng. and the Ph. Dr. degrees from Tsukuba University in 1990, and 2001, respectively. He joined the Central Research Laboratory, Hitachi Ltd. in 1982, where he was involved in the study of integrated solid-state chemical sensor for blood analyses. He was with the Superconducting Sensor

Laboratory from 1991-1996. He was involved in the research and development of SQUID's and multichannel SQUID system. He was with the Central Research Laboratory, Hitachi Ltd. from 1996-2003. He was a Project Leader of the SQUID application research group. He is presently a Professor of Department of Electrical and Electronic Engineering, Okayama University. He is involved in the research of gas sensor and superconducting sensor devices, and their applications.

## Figure captions

Fig. 1. Device structure of the proton pumping gate FET hydrogen gas sensor.

Fig. 2. Measurement circuit.

Fig. 3. Time response curve of the proton pumping gate FET hydrogen sensor with AC rectangular bias voltage from 1 V to -1 V at 0.1 Hz. The hydrogen concentration was changed from  $10^3$  ppm to  $10^4$  ppm at 1 minute. The sensor operated at  $100^\circ\text{C}$  and in a nitrogen atmosphere.

Fig. 4. The DC and AC voltage changes of the proton pumping gate FET hydrogen sensor with the AC rectangular bias voltage. The sensor operated at  $100^\circ\text{C}$  and in a nitrogen atmosphere.

Fig. 5. The DC and AC voltage changes of the proton pumping gate FET hydrogen sensor with AC rectangular bias voltage. The sensor operated at  $100^\circ\text{C}$  and in air.

Table 1. Output voltage changes of the proton pumping gate FET with interference gas concentration. The sensor operated without the bias voltage. The changed gas concentrations are represented in parentheses.

Fig. 6. Nyquist plots of the proton pumping gate at  $100^\circ\text{C}$  in air. The horizontal and longitudinal axes indicate the real and imaginary parts of the impedance respectively. The markers are the measured values and the short dashed lines are drawn as a simulation of the equivalent circuit.

Fig. 7. Resistance changes of the proton pumping gate at  $100^\circ\text{C}$  and in nitrogen.

Fig. 8. Resistance changes of the proton pumping gate at  $100^\circ\text{C}$  and in air.

Table 1

| Gas   | Operating Temperature |       |
|---|-----------------------|-------|
|   | R.T.                  | 100°C |
| O <sub>2</sub> (10 <sup>3</sup> ppm→10 <sup>5</sup> ppm)                | 0 mV                  | -3 mV |
| CH <sub>4</sub> (10 <sup>3</sup> ppm→10 <sup>4</sup> ppm)               | -1 mV                 | -1 mV |
| C <sub>2</sub> H <sub>6</sub> (10 <sup>3</sup> ppm→10 <sup>4</sup> ppm) | 1 mV                  | 6 mV  |
| NH <sub>3</sub> (10 <sup>3</sup> ppm→10 <sup>4</sup> ppm)               | 0 mV                  | 5 mV  |

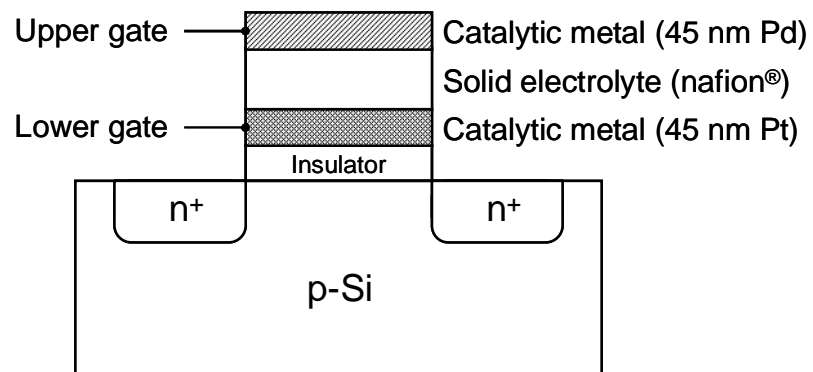


Fig. 1



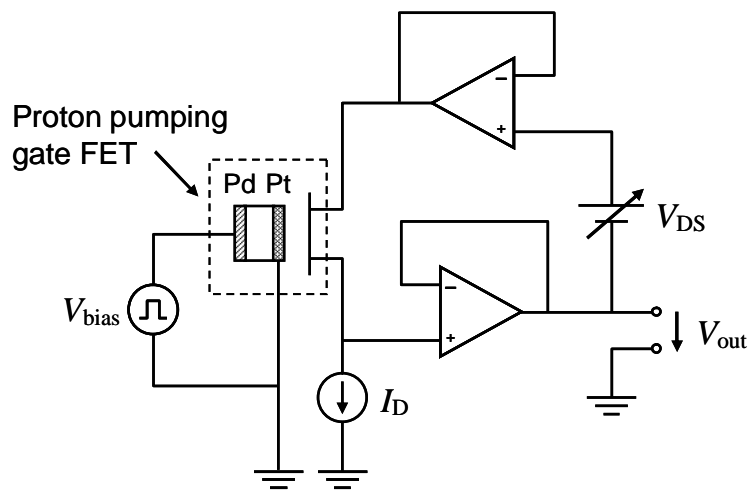


Fig. 2

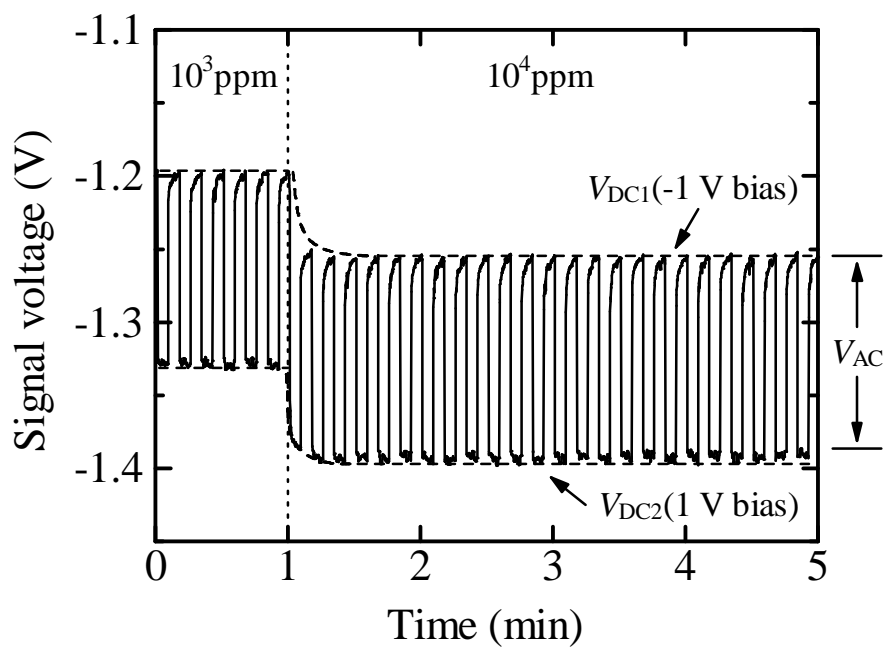


Fig. 3

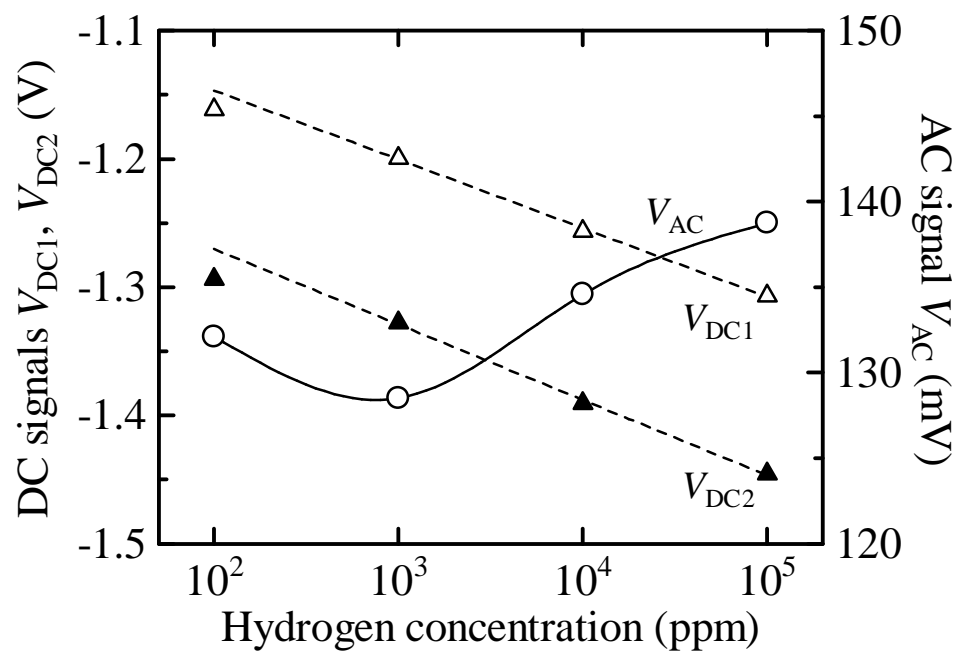


Fig. 4

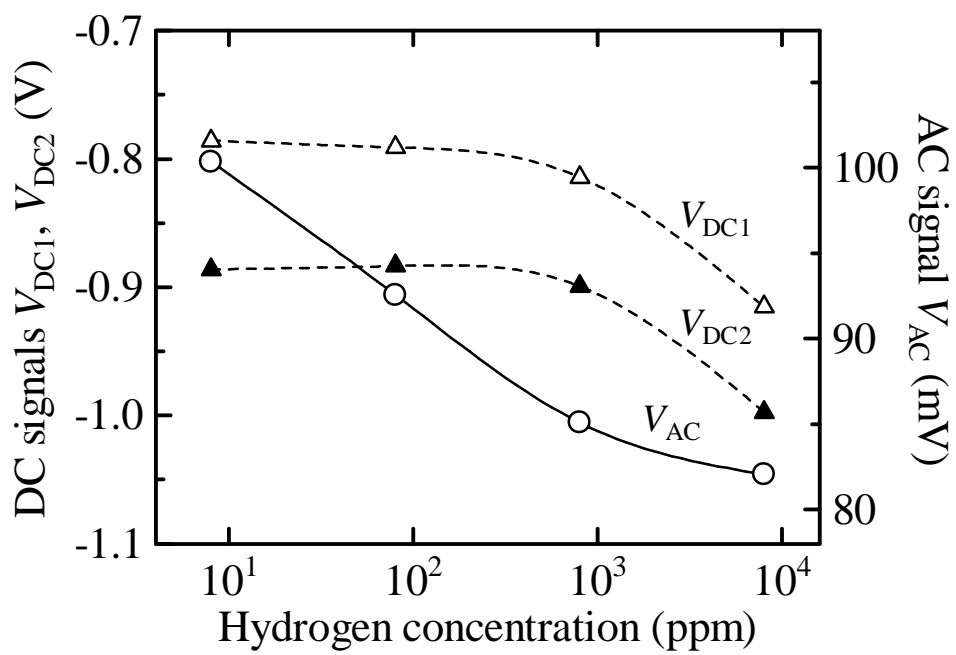


Fig. 5

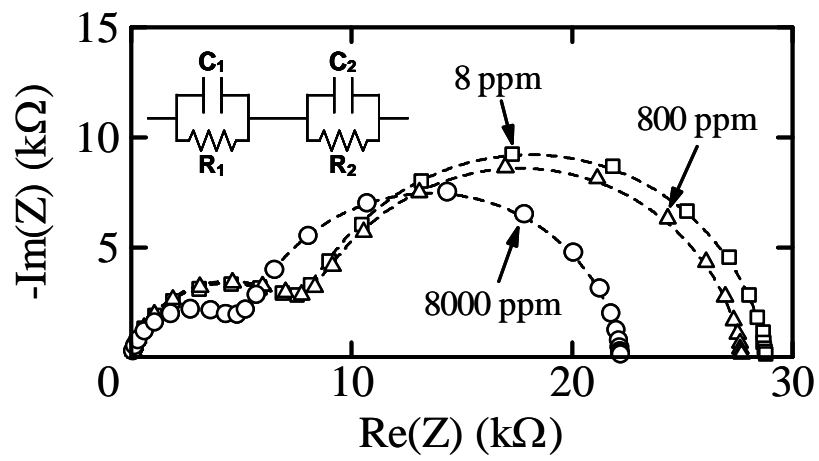


Fig. 6

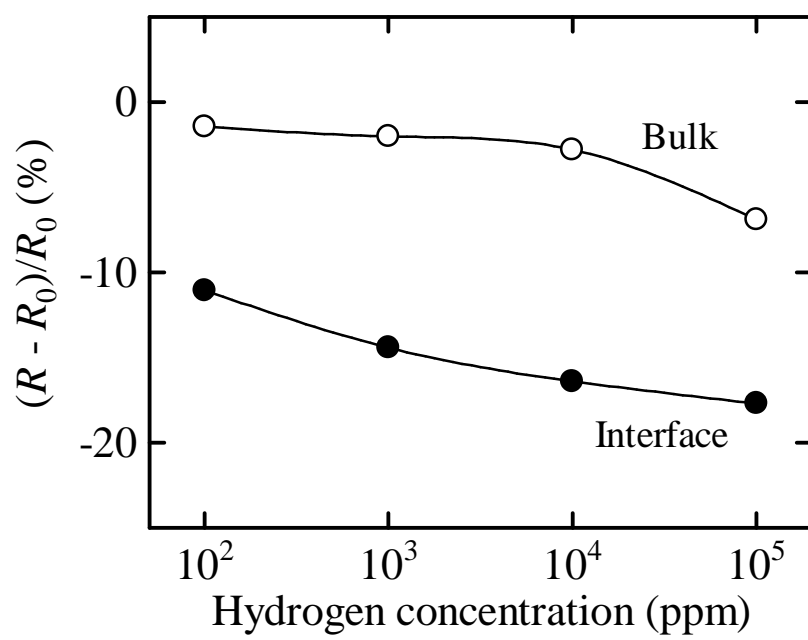


Fig. 7

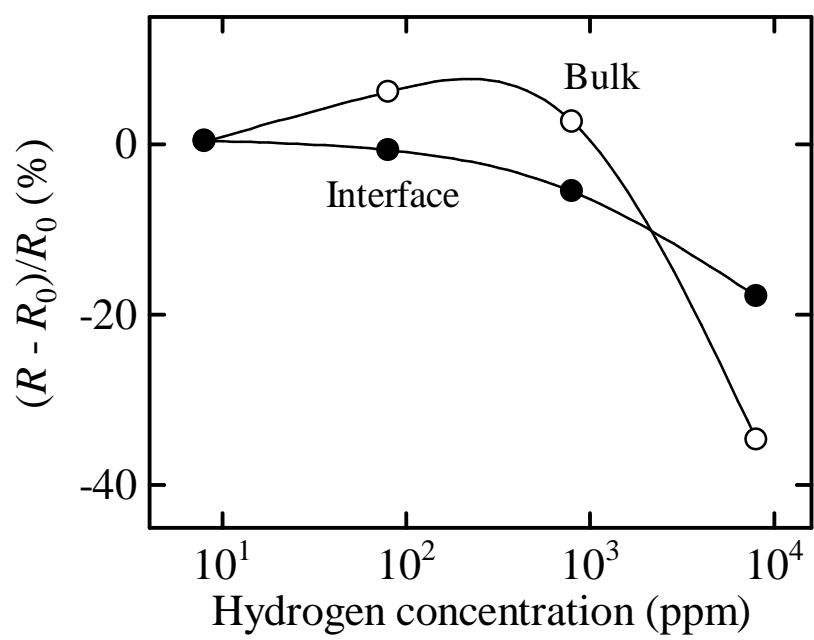


Fig. 8